

Article

# Regional Temporal and Spatial Trends in Drought and Flood Disasters in China and Assessment of Economic Losses in Recent Years

Jieming Chou <sup>1</sup>, Tian Xian <sup>2, \*</sup>, Wenjie Dong and Yuan. Xu

<sup>1</sup> State Key Laboratory of Earth Surface Processes and Resource Ecology, Faculty of Geographical Science, Beijing Normal University, Beijing, China; choujm@bnu.edu.cn

<sup>2</sup> State Key Laboratory of Earth Surface Processes and Resource Ecology, Faculty of Geographical Science, Beijing Normal University, Beijing, China; xiant13@lzu.edu.cn

\* Correspondence: xiant13@lzu.edu.cn

**Abstract:** Understanding the distribution in drought and floods plays an important role in disaster risk management. The present study aims to explore the trends in the standardized precipitation index and extreme precipitation days in China, as well as to estimate the economic losses they cause. We found that in the Northeast China, northern of North China and northeast of Northwest China were severely affected by drought disasters (average damaged areas were 6.44 million hectares) and the most severe drought trend was located in West China. However, in the north of East China and Central China, the northeastern of the Southwest China was severely affected by flood disasters (average damaged areas were 3.97 million hectares) and the extreme precipitation trend is increasing in the northeastern of the Southwest China. In the Yangtze River basin, there were increasing trends in terms of drought and extreme precipitation, especially in the northeastern of the Southwest China, where accompanied by severe disaster losses. By combining the trends in drought and extreme precipitation days with the distribution of damaged areas, we found that the increasing trend in droughts shifted gradually from north to south, especially in the Southwest China, and the increasing trend in extreme precipitation gradually shifted from south to north.

**Keywords:** damaged area; direct economic loss; disaster; drought; extreme precipitation

## 1. Introduction

With global warming, the numbers of extreme precipitation events may increase in many areas [1-3]. Increased frequency of extreme events leads to increased frequency and intensity of floods and droughts, and extreme events have adverse effects on human society and environment [4,5]. Therefore, the studies about extreme events have been attracted more and more attention [6-8].

In recent years (1998–2014), there has been a change from a warming to a cooling trend in the northern region, with a relatively strong warming trend in the Qinghai–Tibet Plateau region and the Southwest China [9]. Increases in atmospheric greenhouse gases warm the surface but they also exacerbate surface evaporation and enhance the ability of the atmosphere to retain Water Vapor, which means that the water content may increase in the atmosphere [10]. Droughts will more likely to occur when the water vapor evaporation increases, to balance the evaporation process, precipitation will also increase and floods will occur. Therefore, precipitation has also changed due to the effects of changes in temperature [11].

Drought is one of the most destructive natural hazards that affect society. Droughts can severely affect agriculture, water resources, ecology, and society [12-14]. Due to recent global warming [15], the percentage of dry regions throughout the world increased by 1.74% per decade from 1950 to

2008 [16]. Drought affects almost everywhere and the potential change is still a major problem. On an annual scale, ENSO (El Nino and Southern Oscillation) is a major factor of drought throughout the Americas, eastern Asia, and Australia [17]. Previous studies have investigated the changes in extreme precipitation events in recent years [18]. It has been shown that extreme precipitation increased significantly in Yangtze River region, Southwest China and South China from 1951 to 2000 [19], with significant increases in heavy rainfall at rural and urban stations in East China [20]. The physical interpretation of extreme precipitation suggested that the western North Pacific subtropical high and mid-latitude wave systems have greatly affected extreme summer precipitation in China [21]. According to Orsolini [22] the Silk Road and polar waves play key roles in regulating extreme precipitation in the north of China and Northeast China. According to regional climate models, the increasing rainstorm days in parts of China is due to the greenhouse [23], the effects of global warming rather than aerosols are considered to be responsible for the heavy rain in eastern China [24].

According to recent statistics, the economic losses caused by global climate change and related extreme climate events have increased by an average of 10 times in the past 40 years. The meteorological disasters accounted for more than 70% of all natural disasters in China [25]. Climate change has direct impacts on increasing the frequency and intensity of extreme events such as droughts and floods, especially in climate-sensitive and vulnerable areas. Since the 1950s, the economic losses caused by droughts and floods have accounted for 78% of all meteorological disasters [26]. To reduce the damage, many studies have investigated drought, flood distribution and propose solutions. Most of these previous studies focused on single disasters, whereas relatively few considered multi-hazard superposition effects. Therefore, in the present study, we used the latest and most unique data to study drought and floods, and considered the characteristics of the East Asian Summer Monsoon Index (EASMI) and the Nino 3.4 index to comprehensively analyze the characteristics of drought and extreme precipitation and the resulting direct economic losses. Thus, we aim to provide better scientific evidence and suggest countermeasures for mitigating and managing the risk of disasters.

**2. Data and Methods**

**2.1 Data**

We used total agricultural output value statistics for various regions from 2000 to 2003 compiled by the National Bureau of Statistics, as well as the drought damaged areas and total planted areas in various regions from 2000 to 2003 from Chinese Agricultural Statistics. The direct economic losses from 2004 to 2015 were derived from the China Meteorological Disaster Yearbook. Daily and monthly precipitation records from 855 stations in China during 2000–2015 were used (Fig. 1). This dataset was obtained from the National Meteorological Administration. Relatively strict quality control was applied before use and stations with short or missing data sequences were deleted. To study the mechanisms responsible for droughts and floods, we also employed the EASMI (<http://ljp.gcess.cn>) defined by Professor Li and the Nino 3.4 index specified by the National Climate Center for Research. For convenience, we divide our domain (China Mainland) into the Northeast China, North China, East China, Central China, South China, Northwest China, and Southwest China (Fig. 2).



Fig. 1 Distribution of meteorological stations.

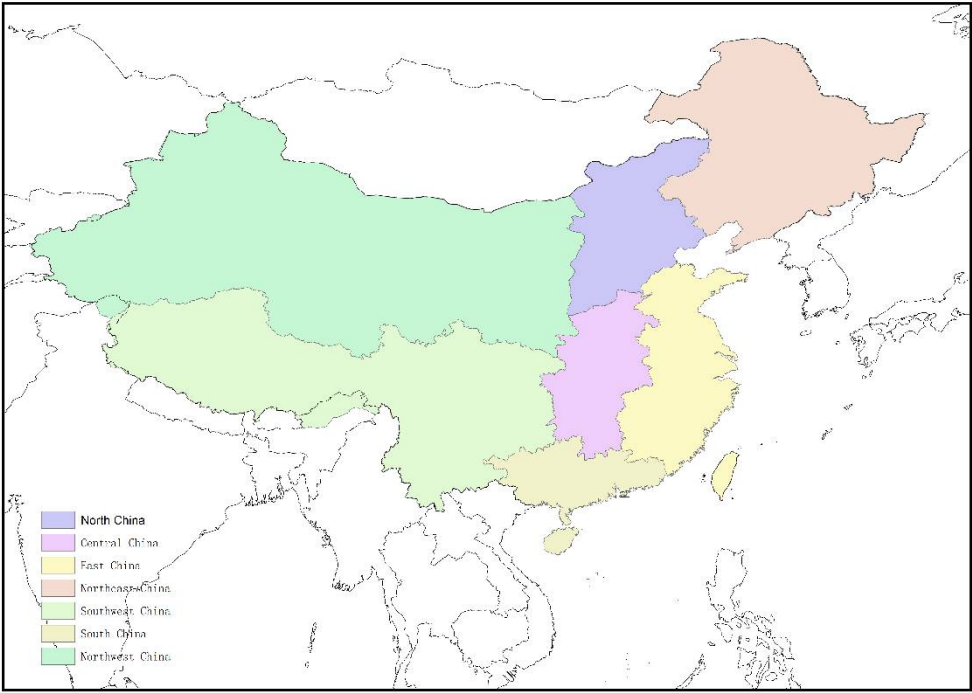


Fig. 2 Devision of sub-regions of research domain.

2.2 Methods

2.2.1 Drought indicators.

We used the standardized precipitation index (SPI) as an indicator of drought. Based on the monthly precipitation data obtained from 855 weather stations in the study area covering 16 years, we analyzed the temporal and spatial features of meteorological drought in the whole research areas by calculating annual time scale SPI (12-month SPI). The mean SPI value at each station is 0. An SPI value > 0 indicates precipitation higher than the mean value in the same period, where the flooding is more severe when the value is larger. An SPI value < 0 indicates that the precipitation is lower than the average level in the same period, where the meteorological drought is more severe when the

value is smaller. The representative drought indicators used throughout the world include the SPI and Z-index. Previous studies indicate that SPI is more stable than the Z-index (Unlike the SPI, Z-index directly normalizes the probability density function), and SPI can meet the requirements of different time scales and analyses of the status of different water resources. A 12-month SPI is a comparison of the precipitation for 12 consecutive months with that recorded in the same 12 consecutive months in all previous years of available data and reflects long-term precipitation patterns [27].

#### 2.2.2 Extreme precipitation indicator.

Frich [28] compiled a new global dataset of derived indicators to clarify whether frequency and severity of climatic extremes changed during the second half of the 20th century. Among them, 5 indicators related to extreme precipitation events were selected: R10(No. of days with precipitation  $\geq 10$  mm d<sup>-1</sup>), CDD (Maximum number of consecutive dry days ( $R_{\text{day}} < 1$  mm)), R<sub>5d</sub> (Maximum 5 d precipitation total), SD II (Simple daily intensity index: annual total/number of  $R_{\text{day}} \geq 1$  mm d<sup>-1</sup>), R95T (Fraction of annual total precipitation due to events exceeding the research period 95th percentile).

In fact, the definitions of extreme precipitation events vary among places. For example, heavy rainfall and heavy rain have never occurred in the history of some stations in Northwest China, but moderate rain often causes landslides and other hazards in this area, and thus defining thresholds according to the criteria for heavy rainfall to study extreme precipitation events has no practical significance. For this reason, percentile-based extreme precipitation index is defined [29]. For a given station, an extreme precipitation event is defined if the daily precipitation is beyond the 95th percentile threshold of all rainy records for the whole 16 years from 2000–2015.

#### 2.3 Estimation method

Due to the lack of data for drought direct economic losses in 2000–2003, the reducing production coefficient method [30–32] was employed to estimate the direct economic losses in these years. This method measures the economic benefits or economic losses due to changes in environmental quality by considering changes in the output value or profit in an area attributable to changes in environmental quality. This method has often been used to calculate the direct crop production losses, economic forest output value losses, timber forest losses, economic losses of grassland resources, and economic losses for fisheries [33]. When the method is used to calculate agricultural losses, it is sometimes called the reducing production coefficient method. This method employs the areas with disasters over the years to estimate agricultural losses and to convert this into the grain output value. Thus, we defined the direct loss due to drought as:

$$Q = \alpha \cdot A \cdot P_q$$

where  $\alpha$  is the agricultural production yield reduction rate,  $P_q$  is the total output value/planted area with crops in each area, and  $A$  is the area affected by the disaster.

#### 2.4 Analysis methods

##### 2.4.1 Empirical Orthogonal Function (EOF)

EOF was used to analyze the direct economic losses due to droughts and floods in China, and the temporal and spatial characteristics of the damaged areas. EOF is a common method for analyzing field sequences [34]. EOF decomposes a certain element field sequence ( $F_{ij}$ ) into an orthogonal time function ( $T_{ih}$ ) and an orthogonal spatial function ( $X_{hj}$ ):

$$F_{ij} = \sum (T_{ih} \times X_{hj}),$$

where  $F_{ij}$  is the factor field,  $i = 1, 2, \dots, m$  is the time sequence number,  $j = 1, 2, \dots, n$  is the station number,  $X_{hj}$  is the spatial function,  $h = 1, 2, \dots, H$  is the decomposed number of fields, and  $T_{ih}$  is a function of time. The spatial function  $X_{hj}$  is usually regarded as a typical field, where it changes completely with space. However, the time function  $T_{ih}$  that only changes with time is considered to be the weight coefficient for a typical field. The EOF generally converges quickly, where the sum of the first few typical fields can represent the actual field, and changes in the time



coefficients reflect the importance of each typical field at different times. The data comprising direct economic losses and damaged areas due to drought and floods met the requirements for EOF analysis. EOF analysis can determine the basic form of the spatial distribution and the time-varying characteristics of drought and flood disasters in China, thereby helping to understand drought and flood disasters in China.

2.4.2 Mann-Kendall test

In this paper, the Mann-Kendall test, which is widely used to detect trends in meteorological data [35]. We estimate temporal changes of the SPI and extreme precipitation days' time series by calculating Mann-Kendall's slope estimator, and we estimate trend significance using the Mann-Kendall test.

2.5 Correlation analysis

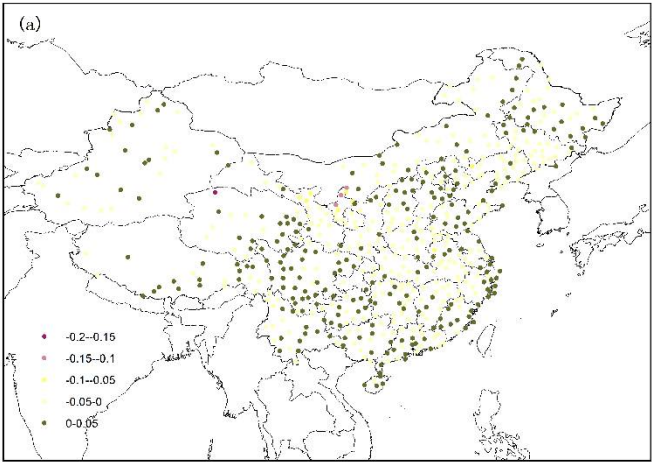
Two climate indices (EASMI and Nino 3.4) were used to analyze the large-scale climate influences on drought and extreme precipitation in China. We evaluated the presence of a statistically significant relationships between SPI/the extreme precipitation days and EASMI/Nino 3.4 by simple linear regression. Significant relationships between drought, the extreme precipitation days, and climate indices were obtained by Pearson regression model. It is noted that climate indices may influence drought and precipitation extremes of the year and the next year [36] but after our observation, the correlation was not significant one year ahead. Therefore, we used EASMI with zero years ahead and Nino 3.4 based on the average in March during the previous year to February in the following year as the candidate predictor variables. Significant relationships were supported when the correlation coefficient differed from zero in the 10% confidence interval.

3 Results and Discussions

3.1 Trends in drought and extreme precipitation

3.1.1 Drought trend

We used the Mann-Kendall test to analyze the trends in SPI based on monthly precipitation data from 2000 to 2015. A negative SPI index indicates a drought trend and the drought level is more obvious when the value is more negative. In Fig. 3b, the yellow dots had relatively negative trends in terms of the SPI coefficient, i.e., clear increases in the drought trend over time. The increasing drought trend was mainly concentrated in the central and western of Southwest China, northern of East China, and Central China. The lowest SPI trend was recorded at Dali Meteorological Station in Yunnan Province. Among the 855 meteorological stations, the drought index exhibited an increasing trend at 34.5% of the stations and there was a decreasing drought trend in most parts of the country.



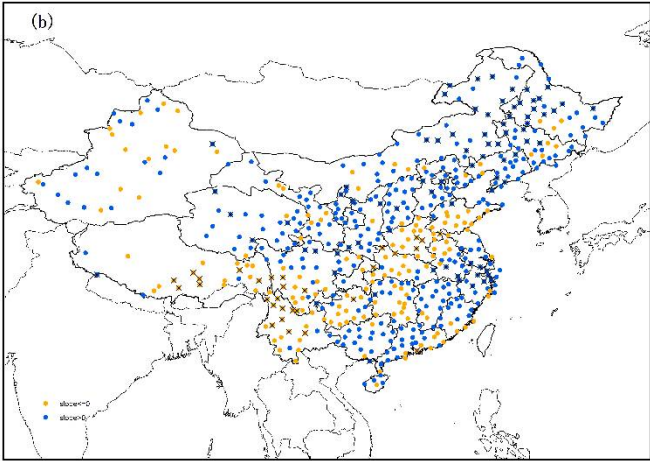
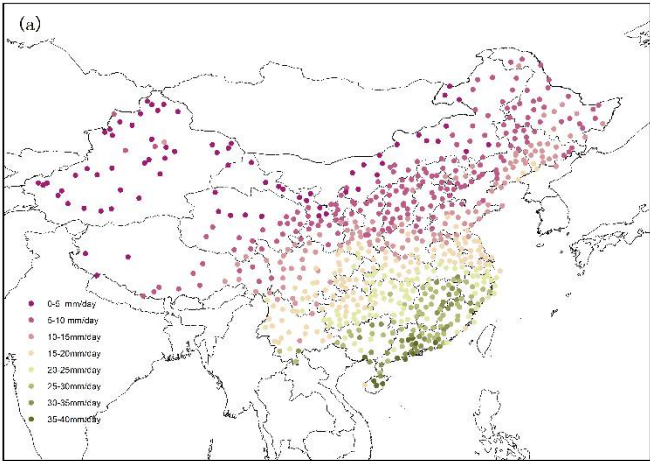


Fig. 3 SPI distribution. (a) Annual average SPI. (b) SPI trend (unit, year-1). The yellow dots indicate that the slope is negative and the drought tend to increase; the blue dots indicate that the slope is positive, and the drought tend to decrease. The point of the cross passed 95% significance test

3.1.2 Extreme precipitation

We used the Mann-Kendall test to analyze the extreme precipitation days' trend based on daily precipitation data recorded in China over 16 years. From 2000 to 2015, the extreme precipitation days tended to increase in Northeast China, North China, northeastern of Southwest China, western of South China, and most of East China (the blue dots in Fig. 4b indicate increases in extreme precipitation). There were obvious increasing extreme precipitation trends in most of the Northeast China, and the central part of the East China. The extreme precipitation tended to increase at 51.7% of the stations, thereby indicating that the extreme precipitation exhibited an increasing trend in most parts of the country due to global warming.



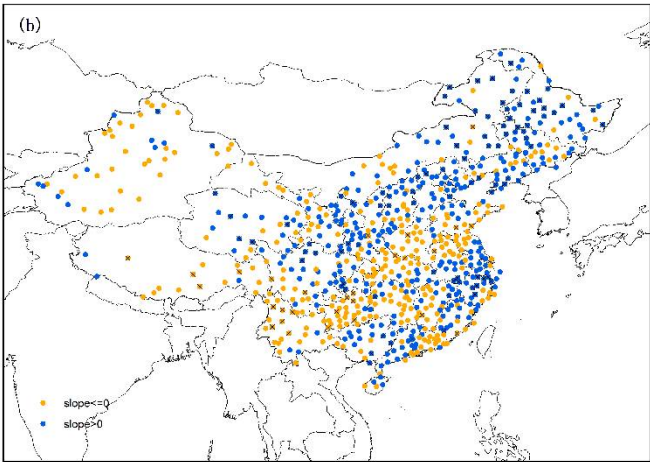


Fig. 4 Extreme precipitation distribution. (a) Annual average extreme precipitation days. (b) extreme precipitation days' trend (unit, year-1). The yellow dots indicate that the slope is negative and the extreme precipitation days tend to increase; the blue dots indicate that the slope is positive, and the extreme precipitation days tend to decrease. The point of the cross passed 95% significance test

3.1.3 Drought and extreme precipitation

Meteorological stations with increasing trends in terms of both the regional drought and extreme precipitation were selected to characterize the superposition effect of them in space (red dots in Fig. 5). The areas with increases in SPI and extreme precipitation were concentrated mainly in the Yangtze River basin, especially the middle and upper reaches of the Yangtze River. For this special phenomenon, may be P-E pattern could explain [37]. Wet regions get wetter and dry regions drier When water vapor is not restricted. The Yangtze River is the boundary between dry and wet, and due to its ample water vapor conditions it would wetter and drier too.

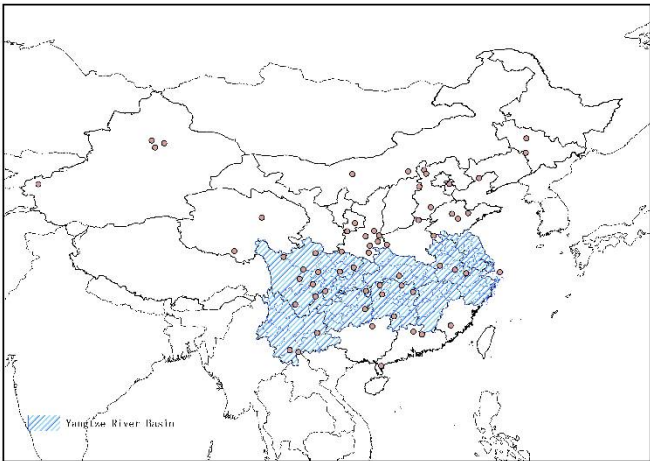


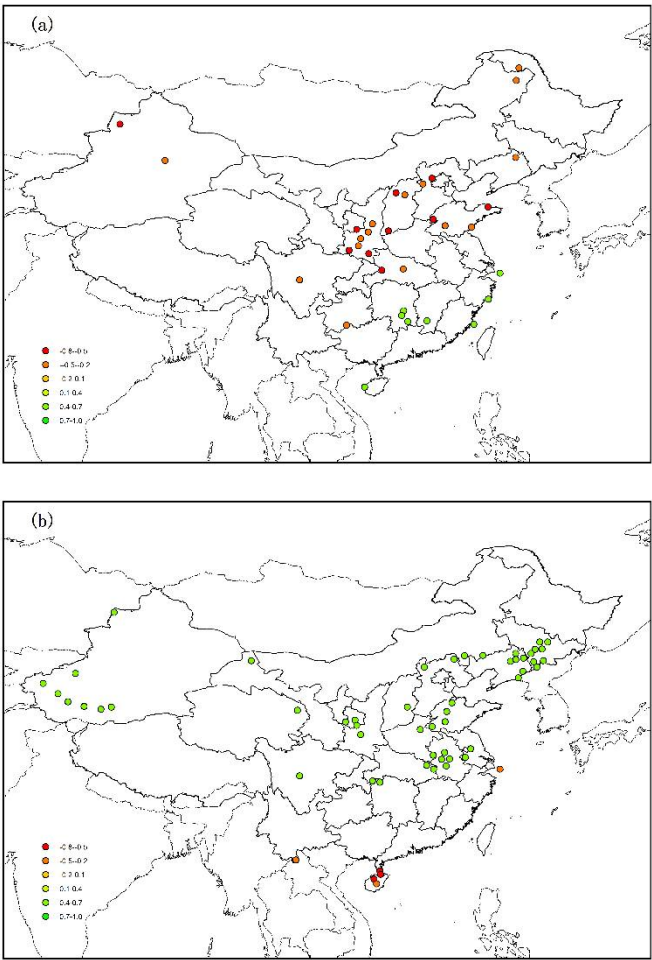
Fig. 5 Superimposed distributions of drought and extreme precipitation. Red dots are used to indicate stations with increased drought and extreme precipitation

3.2 Correlation analysis

The Yangtze River Basin is an important agricultural area in China and a region with rapid economic development. However, obvious changes have occurred in the annual precipitation during the flood season in the Yangtze River valley, where drought and flood disasters are more frequent [38,39]. Climate disasters often cause great damage and losses to local industry and

agriculture, as well as affecting the safety of people and property. According to 3.1, the frequencies of drought and floods have increased in recent years in the Yangtze River basin. Therefore, we focused on the correlation between the Yangtze River basin and the climate index.

Figure 6 shows the correlations between drought, extreme precipitation frequency, and the two climate indices comprising EASMI, Nino 3.4. In general, only a few stations had significant correlations with EASMI and Nino 3.4. However, some spatial characteristics still could be identified. SPI was significantly positively correlated with EASMI with zero years ahead mainly in the middle and lower reaches of the Yangtze River, thereby indicating that the frequency of drought in the middle and lower reaches of the Yangtze River will increase when the East Asian summer monsoon weakens. In the northern of the Yangtze River, SPI and Nino 3.4 were significantly positively correlated, which indicates that when the sea surface temperature (SST) decreases in the tropical eastern Pacific, the drought will increase in the northern of the Yangtze River, i.e., drought will occur in La Nina years. It is worth noting that the SST in the tropical eastern Pacific will affect most northern regions. In the southern part of the Yangtze River basin, the extreme precipitation days were significantly positively correlated with EASMI. Thus, extreme precipitation will increase in the southern part of the Yangtze River basin when the East Asian summer monsoon increases. By contrast, the extreme precipitation days were significantly negatively correlated with EASMI in the northern of the Yangtze River, so when the East Asian summer monsoon increases, extreme precipitation will weaken in this area. The extreme precipitation days were significantly positively correlated with Nino 3.4 in most areas of the Yangtze River basin, thereby indicating that extreme precipitation will increase in the Yangtze River basin when the SST in the tropical eastern Pacific rises. Thus, extreme precipitation will increase in the Yangtze River basin during El Niño years.





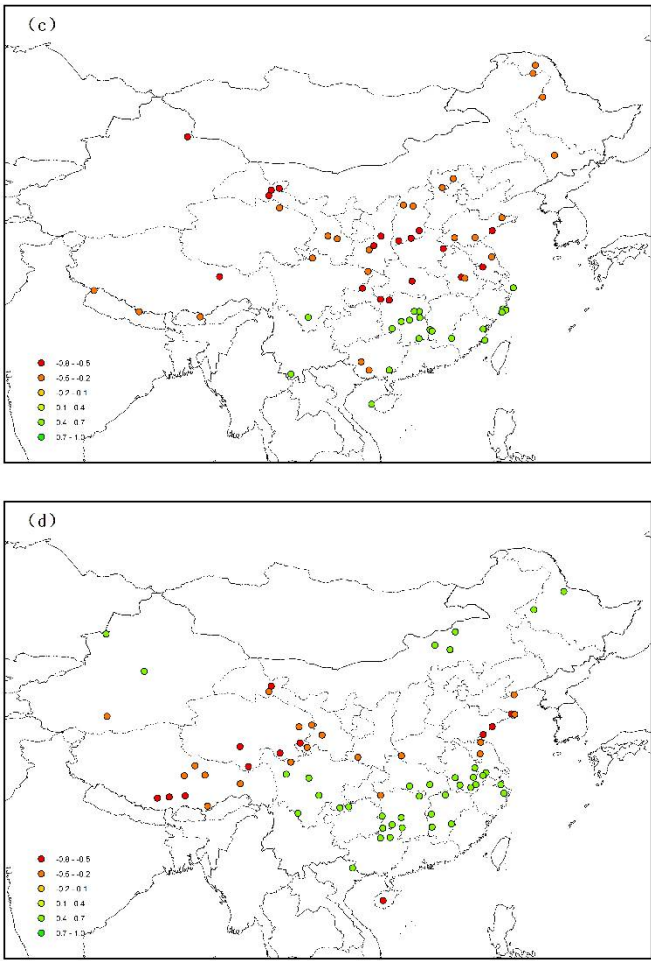


Fig. 6 Statistical correlations between SPI, extreme precipitation days, and EASMI, Nino 3.4. Correlations between: (a) SPI and EASMI, (b) SPI and Nino 3.4, (c) extreme precipitation frequency and EASMI, (d) extreme precipitation frequency and Nino 3.4.

### 3.3 Disasters Analysis

#### 3.3.1 Spatial and temporal distributions of drought losses

Figure 7 shows the EOF first mode distribution for the drought direct economic loss anomaly field in China during the 16-year period. The contribution of the first mode's variance was 36.9%, which reflects the main characteristics of the spatiotemporal changes in the direct economic losses. The first dimension of the direct economic loss anomaly exhibited a downward trend from northeast to southwest, thereby indicating that the drought economic losses decreased gradually from northeast to southwest, where the high value areas were located in the southeast of Northeast China and north of East China (Their average direct economic losses amounted to RMB 13.8 billion and accounted for 18.6% of all regions). During midsummer, the daytime is often longer than the night in the Northeast China, and the sunshine duration is long, thereby resulting in high evaporation and the rapid onset of drought. In the spring, there is less precipitation in the Northeast China, and low precipitation but high evaporation in the summer, thereby leading to continuous drought. After 2000, droughts occurred frequently in Northeast China and these droughts lasted for a long time. There were two consecutive dry periods in 2000–2002 and 2007–2008. In terms of the spatial distribution, 2000–2010 was the period with the highest frequency and effect of drought in the Northeast China, especially in the central and western parts of them, where the drought frequency reached 42.86% and 33.34%, respectively [40]. In addition, a comparison of the first EOF pattern in the area affected by drought in Fig. 8 shows that the spatial distribution of the agricultural

damaged areas were roughly consistent with the spatial distribution of the direct economic losses, where it decreased gradually from the northeast to the southwest (where the high-value areas were located in Northeast China and Inner Mongolia, with an average damaged area of 6.44 million hectares and accounted for 31.6% of the total), and thus agricultural losses accounted for a large proportion in direct economic losses. When we compared Heilongjiang and Shandong, we found that the Heilongjiang's damage areas were severe while the economic losses were low, and Shandong has oppositethe. Shandong is a large agricultural province and its agricultural output is higher than that of Heilongjiang. Therefore, the economic losses could be high even when a drought was not particularly severe.

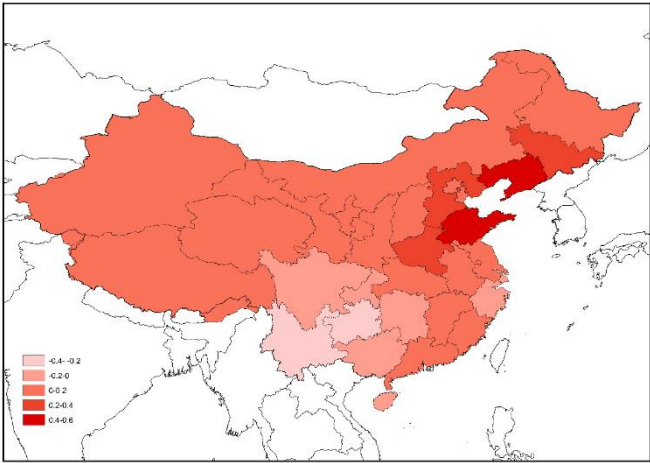


Fig. 7 First mode of EOF for the drought direct economic loss anomaly field.

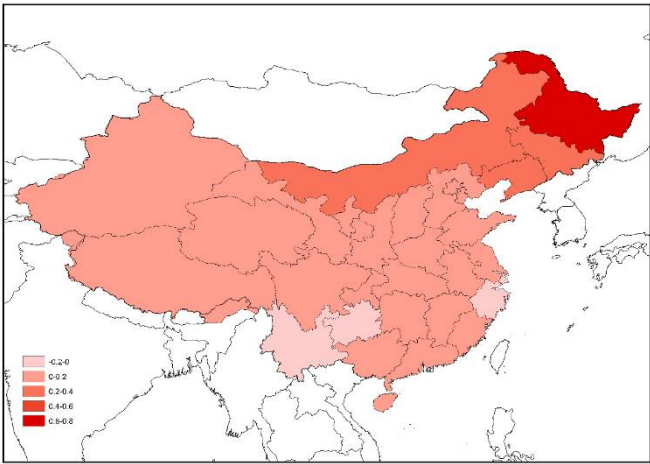


Fig. 8 First mode of EOF for the drought damaged areas anomaly field.

The time coefficient of direct economic losses due to drought in Fig. 9a show that the losses in 2000–2003, 2007, 2009, and 2014 were all greater than the average, and the losses continued to increase in 2005–2007. In the drought damaged areas (Fig. 9b), the losses in 2000–2004, 2006–2007, and 2009 were all greater than the average, and the area affected by disasters increased continuously in 2005–2007. The two graphs in Fig. 9 show that the changing in the economic losses was generally consistent with the changing in the affected area. However, 2003 and 2014 were rather exceptional. In 2003, the damaged areas were relatively large but the economic losses were relatively small. By contrast, the affected area was small and the economic losses were relatively large in 2014. These findings may be explained by the contribution rate of primary industry to GDP was low in 2003 and high in 2014.

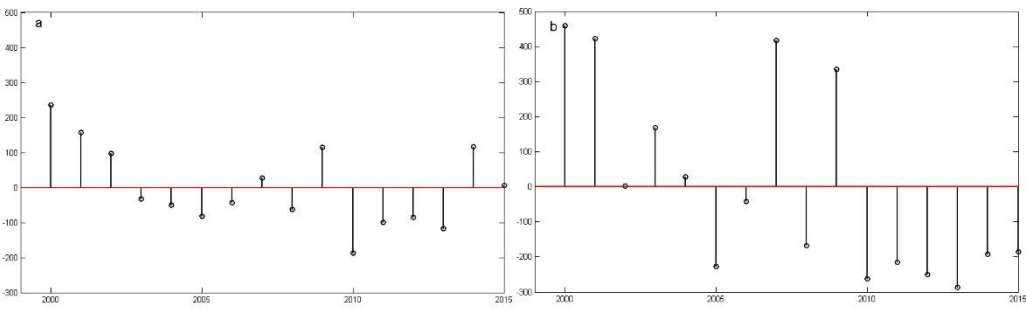


Fig. 9a Time coefficient of drought direct economic loss anomalies. b Time coefficient of drought damage areas anomalies.

3.3.2 Spatial and temporal distributions of flood losses

Figure 10 shows the EOF first mode distribution for the flood direct economic loss anomaly field in China during the 16-year period. The contribution of the first mode's variance was 56.8%, which reflects the main characteristics of the spatiotemporal changes in the direct economic losses. Fig. 10 clearly shows the abnormal flood losses in the southeast of Northeast China, northeast of Southwest China and Central China (Their average direct economic losses amounted to RMB 56.7 billion and accounted for 51.1% of all regions). However, compared with Fig. 11, the anomalous flood damaged areas were larger in the northeast of Southwest China, north of Central China and East China (with an average damaged area of 3.97 million hectares and accounted for 43% of the total). These anomalous results may be explained by the inadequate defenses against storms and floods in Northeast China and southwestern parts of East China, whereas the central areas of East China and northern parts of Central China were more resistant to heavy rainfall. In addition, these results reflected the fact that the direct economic losses caused by floods were due to other economic losses as well as agricultural losses. "Managing the Risks of Extreme Events and Disasters to Advance Climate Change Adaptation" issued by the IPCC (Intergovernmental Panel on Climate Change) specifically states that the impacts of extreme and non-extreme events, and whether they constitute disasters, depends on the level of exposure and vulnerability as well as the strength of the event itself. Exposure and vulnerability are key decisions when assessing the risk of disaster and its impact. The top 10 provinces in terms of the annual multi-year average disaster exposure were Hubei, Anhui, Hunan, Henan, Jiangsu, Heilongjiang, Jilin, Jiangxi, Sichuan, and Shandong, as shown in Figs 10 and 11. The extremely severe disaster losses in Sichuan, Jilin, and Jiangxi may also have been caused by the high disaster exposure levels of these provinces.

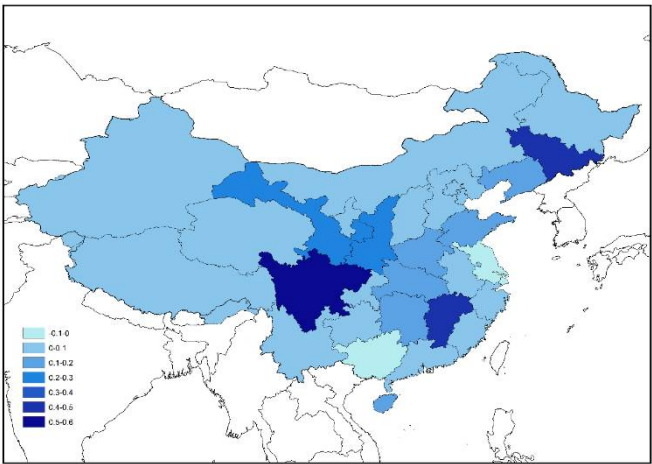


Fig. 10 First mode of EOF for the flood direct economic loss anomaly field.

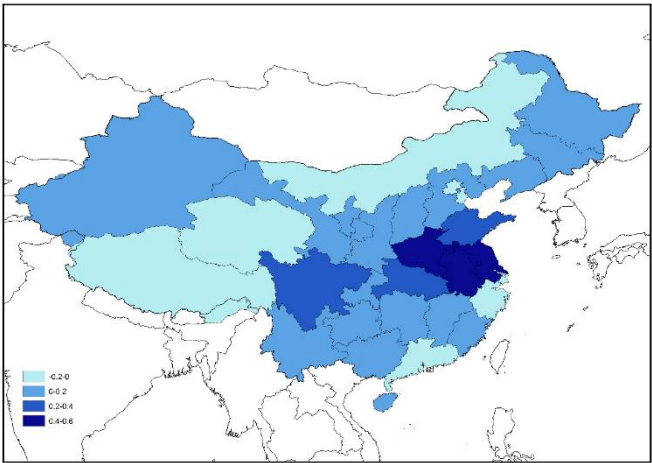


Fig. 11 First mode of EOF for the flood damaged areas anomaly field.

The time coefficient charts in Fig.12 show that 2010 was a year with particularly severe flooding disasters, including flood damaged areas and direct economic losses. However, the maximum area affected by rainstorms and floods occurred in 2003 during the study period, but the direct economic losses were not severe. The reason for this difference is explained in Section 3.3.1.

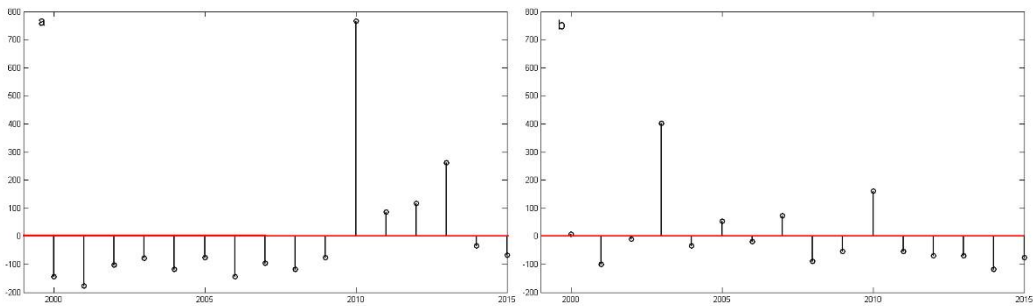


Fig. 12a Time coefficient of flood direct economic loss anomalies. b Time coefficient of flood damaged area anomalies.



4. Concluding remarks

Based on the results obtained in this study, we can give the following main conclusions.

- (1) In recent years, 34.5% of the country's meteorological stations have experienced increasing trends in drought, which were mainly concentrated in the southern of Southwest China, northern of East China and Central China.
- (2) Due to global warming, extreme precipitation has also become more frequent, especially in the Northeast China, the eastern of the Northwest China, and the central region of East China.
- (3) Special climate phenomena have been observed in the Yangtze River basin due to its special circulation characteristics and geographical location. Meteorological disasters have occurred frequently in recent years in the Yangtze River basin, where the frequencies of both drought and extreme precipitation have increased (Fig. 5). The northeastern of the Southwest China has been particularly severely affected, with severe drought damaged areas and flood damaged areas.
- (4) Comparisons of the drought trend distribution (Fig. 3b) and drought damaged areas (Fig. 8) showed that the drought damaged areas were relatively severe in the north of East China and Central China, and the drought will increase in these areas. Therefore, it is necessary to increase defense and control measures to prevent drought disasters in these regions.
- (5) Comparisons of the extreme precipitation trend distribution (Fig. 4b) and flood damaged areas (Fig. 12) showed that the flood damaged areas were relatively severe in the southern of East China, and the frequency of extreme precipitation also increased in most of these areas. Therefore, it is necessary to increase defense and control measures to prevent flood disasters in these regions.
- (6) The Northeast China has been greatly affected by the drought but the drought trend is weakening (Fig. 3) whereas extreme precipitation (Fig. 4) has tended to increase. Thus, extreme precipitation has shifted to the north with less drought, and the frequency of extreme precipitation may increase. However, the north of East China and Central China have been affected by severe floods, but the drought trend is increasing (Fig. 3) and extreme precipitation (Fig. 4) is decreasing, thereby indicating that drought is shifting to the south with less floods, but the possibility of more severe drought.

**Author Contributions:** conceptualization, Chou. jieming. and Dong. wemjie; methodology, Xian. tian.; software, Xian. tian.; validation, Xian. tian.; formal analysis, Xian. tian.; investigation, Xian. tian.; resources, Xian. tian.; data curation, Xu. yuan.; writing—original draft preparation, Xian. tian.; writing—review and editing, Xian. tian.; visualization, Xian. tian.; supervision, Xian. tian.; project administration, Chou. jieming; funding acquisition, Chou. jieming.

**Funding:** This work was supported by National Key Research and Development Program of China (grant 2016YFA0602703), National Natural Science Foundation of China (grant 41575001), Skate Key Laboratory of Earth Surface Processes and Resource Ecology Project (2017-FX-03), and Supported Scientific Research Foundation Beijing Normal University (2015KJJCA14).

**Acknowledgments:** Thanks to the "International Science Editing" for helping us to polish this article.

**Conflicts of Interest:** No conflict of interest exists in the submission of this manuscript, and manuscript is approved by all authors for publication.

References

- Allen, M. R., Ingram, W. J. Constraints on future changes in the hydrological cycle, *Nature* **2002**, *419*, 224–232
- Alley, R. B., Marotzke, J., Nordhaus, W. D., Overpeck, J. D., Peteet, D. M., Pielke, R. A., et al. Abrupt climate change. *Science* **2003**, *299*(5615), 2005–2010

3. IPCC. Climate Change 2013: The Physical Science Basis. Contribution of Working Group I to the Fifth Assessment Report of the Intergovernmental Panel on Climate Change. Cambridge University Press **2013**, Cambridge and New York.
4. Orsolini, Y. J., Zhang, L., Peters, D. H. W., Fraedrich, K., Zhu, X., Schneidereit, A., et al. Extreme precipitation events over north China in August 2010 and their link to eastward-propagating wave-trains across Eurasia: observations and monthly forecasting. *Quart. J. Roy. Meteor. Soc* **2016**, *141*, 3097–310, doi:10.1002/qj.2594
5. Deng, Y., Jiang, W. G., He, B., Chen, Z., Jia, K. Change in Intensity and Frequency of Extreme Precipitation and its Possible Teleconnection With Large-Scale Climate Index Over the China From 1960 to 2015. *J. Geophys. Res-Atmos* **2018**, *123* (4), <https://doi.org/10.1002/2017JD027078>
6. Zhai, P., Zhang, X., Wan, H., Pan, X. Trends in total precipitation and frequency of daily precipitation extremes over China. *J. Clim* **2005**, *18*, 1096–1108
7. Hoerling, M., Kumar, A., Dole, R., Nielsengammon, J. W., Eischeid, J., Perlwitz, J. Anatomy of an extreme event, *J. Clim.* **2013**, *26*, 2811–2832, doi:10.1175/JCLI-D-12-00270.1
8. Popovicheva, O., Kistler, M., Kireeva, E., Persiantseva, N., Timofeev, M., Kopeikin, V., et al. Physicochemical characterization of smoke aerosol during large-scale wildfires: Extreme event of August 2010 in Moscow. *Atmos. Environ* **2014**, *96*(7), 405–414, doi: 10.1016/j.atmosenv.2014.03.026
9. Xu, Y., Tang, G. L., Zhang, Q. Analysis of the Variation of the Air Temperature over China During the Global Warming Hiatus Period. *Clim. Chang. Res* **2017**, *6*, 569–577
10. Willett, K. M., Gillett, N. P., Jones, P. D., Thorne, P. W., Attribution of observed surface humidity changes to human influence. *Nature* **2007**, *449*, 710–712, doi:10.1038/nature06207
11. Trenberth, K. E. Atmospheric moisture residence times and cycling: Implications for rainfall rates and climate change. *Climatic Change* **1998**, *39*, 667–694.
12. Mishra, A. K., Singh, V. P. A review of drought concepts, *J. Hydrol* **2010**, *391*, 202–216, doi: 10.1016/j.jhydrol.2010.07.012
13. Lei, T. J., Pang, Z., Wang, X., Li, L., Fu, J., Kan, G., et al. Drought and carbon cycling of grassland ecosystems under global change: a review. *Water* **2016**, *8*, 460, doi:10.3390/w8100460
14. Schubert, S. D., Stewart, R. E., Wang, H., Barlow, M., Berbery, E. H., Cai, W., et al. Global meteorological drought: A synthesis of current understanding with a focus on SST drivers of precipitation deficits. *J. Clim* **2016**, *29*, 3989–4019
15. IPCC. Climate Change 2013: The Physical Science Basis. Contribution of Working Group I to the Fifth Assessment Report of the Intergovernmental Panel on Climate Change. Cambridge University Press **2013**, Cambridge and New York.
16. Dai, A. Increasing drought under global warming in observations and models, *Nat. Clim. Chang* **2013**, *3*, 52–58, doi:10.1038/nclimate1633
17. Schubert, S. D., Stewart, R. E., Wang, H., Barlow, M., Berbery, E. H., Cai, W., et al. Global meteorological drought: A synthesis of current understanding with a focus on SST drivers of precipitation deficits. *J. Clim* **2016**, *29*, 3989–4019, doi:10.1175/JCLI-D-15-0452.1
18. Zhang, D. Q., Feng, G. L., Hu, J. G. Trend of extreme precipitation events over China in last 40 years. *Chin. Phys. B* **2008**, *17*, 736, doi:10.1088/1674-1056/17/2/062
19. Zhai, P., Zhang, X., Wan, H., Pan, X. Trends in total precipitation and frequency of daily precipitation extremes over China. *J. Clim* **2005**, *18*, 1096–1108, doi:10.1175/JCLI-3318.1
20. Liu, R., Liu, S. C., Cicerone, R. J., Shui, C. J., Li, J., Wang, J. L., et al. Trends of extreme precipitation in eastern China and their possible causes. *Adv. Atmos. Sci* **2015**, *32*, 1027–1037, doi:10.1007/s00376-015-5002-1
21. Li, J., Wang, B. Predictability of summer extreme precipitation days over eastern China. *Clim. Dyn* **2017**, *1*–12, doi:10.1007/s00382-017-3848-x
22. Orsolini, Y. J., Zhang, L., Peters, D. H. W., Fraedrich, K., Zhu, X., Schneidereit, A., et al. Extreme precipitation events over north China in August 2010 and their link to eastward-propagating wave-trains across Eurasia: observations and monthly forecasting. *Quart. J. Roy. Meteor. Soc* **2015**, *141*, 3097–3105
23. Gao, X., Zhao, Z., Filippo, G. Changes of extreme events in regional climate simulations over East Asia. *Adv. Atmos. Sci* **2002**, *19*, 927–942
24. Liu, R., Liu, S. C., Cicerone, R. J., Shui, C. J., Li, J., Wang, J. L., et al. Trends of extreme precipitation in eastern China and their possible causes. *Adv. Atmos. Sci* **2015**, *32*, 1027–1037

25. Jiang, Z. H., Ding, Y. G., Chen, W. L. Projection of Precipitation Extremes for the 21st Century over China. *Adv. Clim. Chang. Res* **2007**, *3*, 202-207
26. Huang, R. H., Zhou, L. T. Research on the characteristics, formation mechanism and prediction of severe climatic disasters in China, *J Nat Disaster* **2002**, *11*, 1-9
27. Richard, R., Heim, J. A Review of Twentieth-Century Drought Indices Used in the United States. *Arid. Meteorol* **2006**, *24*, 79-89, doi:10.1175/ 1520-0477-83.8.1149
28. Frich, P., Alexander, L. V., Della-Marta, P., Gleason, B., Haylock, M., Klein Tank, A. M. G., Peterson, T. Observed coherent changes in climatic extremes during the second half of the twentieth century, *Clim. Res* **2002**, *19*(3), 193-212. doi:10.3354/cr019193
29. Alexander, L. V, Zhang, X., Peterson, T. C., Caesar, J., Gleason, B., Klein Tank, A. M. J., et al. Global observed changes in daily climate extremes of temperature and precipitation, *J. Geophys. Res. Atmos* **2006**, *111*: D05109
30. Doorenbos, J., Kassam, A. H., Branscheid, V., Bentvelsen, C.L.M. Yield response to water. *Irrigation & Agricultural Development* **1986**, *33*(6), 257-280
31. Shen, P. G., Zhao, B. Y. Discussion on Calculation Method of Economic Loss of Drought Disaster. *Journal of Economics of Water Resources* **1994**, *2*, 15-18
32. Xie, Y. G., Yuan, L. L., Sun, Y. N. Influence of natural disasters on peasant- households' economy and households' withstanding capacity. *J. Nat. Disaster* **2007**, *16*, 171-179
33. Gan, L. J., Xiang, Y., Tian, X. R. The probing of drought-flood disaster in Jiangshu province on the evaluation of crop economic loss. *Scientia. Meteor. Sinica* **2001**, *1*, 122-126
34. Baldwin, M. P., Stephenson, D. B., Jolliffe, I. T. Spatial weighting and iterative projection methods for EOFs. *J. Clim* **2009**, *22*, 234-243
35. Hamed, K. H., Trend detection in hydrologic data: the Mann-Kendall trend test under the scaling hypothesis. *J. Hydrol* **2008**, *349*, 350-363, doi: 10.1016/j.jhydrol. 2007. 11. 009
36. Xiao, M., Zhang, Q., Singh, V. P. Spatiotemporal variations of extreme precipitation regimes during 1961–2010 and possible teleconnections with climate indices across China. *Int. J. Climatol* **2017**, *37*, 468–479, doi:10.1002/joc.4719
37. Held, I. M., Soden, B. J. Robust Responses of the Hydrological Cycle to Global Warming, *J. Clim* **2005**, *19*, 5686-5699, doi:10.1175/JCLI3990.1
38. Huang, R. H., Kumar, A., Dole, R., Nielsengammon, J. W., Eischeid, J., Perlwitz, J., et al. A comprehensive method for seasonal prediction of drought and flood and the seasonal and overseasonal prediction experiments for the summers of 1991 ~ 1995. *Climatic. Environ. Res* **1997**, *2*, 1-15
39. Liu, Y. X., Zhao, Z. G.Y., Zhu, F., Wang, J. P., Chen, L. H. Research of JJA Precipitation Anomaly in Yangtze River Basin Since 2000. *Plat. Meteorol* **2008**, *27*, 807-813
40. Sun, B. F., Zhao, H., & Wang, X. K. Spatiotemporal Characteristics of Drought in Northeast China Based on SPEI. *Ecol. Environ* **2015**, *1*, 22-28